Steel and Composite Structures, *Vol. 25, No. 1 (2017) 79-92*
DOI: https://doi.org/10.12989/scs.2017.25.1.079

Shear capacity of stud shear connectors with initial damage: Experiment, FEM model and theoretical formulation

Jianan Qi [1,2a], Jingquan Wang [*1], Ming Li [1b] and Leilei Chen [1b]

[1] *Key Laboratory of Concrete and Prestressed Concrete Structures of Ministry of Education, Southeast University, Nanjing 210096, China*
[2] *Department of Civil & Environmental Engineering, University of Tennessee-Knoxville, Knoxville, TN, USA*

(*Received May 25, 2016, Revised June 11 2017, Accepted June 17, 2017*)

Abstract. Initial damage to a stud due to corrosion, fatigue, unexpected overloading, a weld defect or other factors could degrade the shear capacity of the stud. Based on typical push-out tests, a FEM model and theoretical formulations were proposed in this study. Six specimens with the same geometric dimensions were tested to investigate the effect of the damage degree and location on the static behavior and shear capacity of stud shear connectors. The test results indicated that a reduction of up to 36.6% and 62.9% of the section area of the shank could result in a dropping rate of 7.9% and 57.2%, respectively, compared to the standard specimen shear capacity. Numerical analysis was performed to simulate the push-out test and validated against test results. A parametrical study was performed to further investigate the damage degree and location on the shear capacity of studs based on the proposed numerical model. It was demonstrated that the shear capacity was not sensitive to the damage degree when the damage section was located at 0.5d, where d is the shank diameter, from the stud root, even if the stud had a significant reduction in area. Finally, a theoretical formula with a reduction factor K was proposed to consider the reduction of the shear capacity due to the presence of initial damage. Calculating K was accomplished in two ways: a linear relationship and a square relationship with the damage degree corresponding to the shear capacity dominated by the section area and the nominal diameter of the damaged stud. This coefficient was applied using Eurocode 4, AASHTO LRFD (2014) and GB50017-2003 (2003) and compared with the test results found in the literature. It was found that the proposed method produced good predictions of the shear capacity of stud shear connectors with initial damage.

Keywords: studs; initial damage; push-out test; shear capacity; reduction factor; FEM analysis

1. Introduction

In recent decades, steel-concrete composite bridges have been widely used in the construction of urban bridges due to their economical and structural advantages (Nie and Cai 2003, Xue *et al*. 2008, Xu *et al*. 2014, Xing *et al*. 2016). Stud shear connectors are typically used as common shear connectors in steel-concrete composite bridges to transfer longitudinal shear force at the interface between steel and concrete (Salari *et al*. 1998, Ju and Zeng 2015, Pathirana *et al*. 2015, Han *et al*. 2017). However, damage to stud shear connectors are typically found in existing bridges. The initial damage to a stud due to corrosion, fatigue, unexpected overloading, a weld defect and other factors could degrade the serviceability and, occasionally, even threaten the safety and service life of steel and concrete composite structures. Therefore, reliability assessment of initially damaged stud shear connectors is significant when evaluating the safety of an entire composite structure.

A push-out test is an efficient tool to evaluate the shear behavior and capacity of stud shear connectors due to its low cost and short duration. Currently, a significant amount of experimental tests have been reported in the literature to investigate the shear behavior of push-out test specimens over many dacades (Viest 1956, Oehlers 1989, Pallarés and Hajjar 2010, Liu and Alkhatib 2013, Xu *et al*. 2014, Su *et al*. 2014). Unfortunately, relatively scarce research on the effect of the initial damage on the behavior of a stud is available in the literature.

Oehlers and Park (1992) carried out an experimental study of shear studs with longitudinally cracked concrete slabs and noted that the initial damage of the longitudinal cracks on the concrete slabs reduced the shear strength of the associated shear connectors. Xu and Sugiura (2013) performed a numerical simulation analysis on group studs shear connector under effect of bending-induced concrete cracks. Their parametric analysis results demonstrated that bending-induced concrete slabs caused a reduction in the stud shear stiffness but had no significant influence on the shear capacity. Rong *et al*. (2013) executed fifteen push-out tests to investigate the effect of corrosion on the static behavior of studs and found that corrosion could result in a significant reduction in the studs' shear capacity. Generally, it is significant that most of these studies rarely gained attention on the effects of initial damage on studs in detail.

To theoretically calculate the shear capacity of stud shear connectors, many studies proposed some computational formulas (Viest 1956, Slutter and Driscoll

*Corresponding author, Professor,
E-mail: wangjingquan@seu.edu.cn
[a] Ph.D. Student, E-mail: qijianan723@126.com
[b] Graduate student

ISSN: 1229-9367 (Print), 1598-6233 (Online)

1965, Goble 1968, Ollgaard *et al*. 1971, Hiragi *et al*. 1989, Xue *et al*. 2008). However, it is worth thinking whether these methods would applicable to evaluate the shear capacity of studs with initial damage. Actually, damage to studs should result in a decline of their shear capacity based on intuitive judgment. Therefore, a theoretical formula is required to accurately predict the shear bearing capacity of studs.

This paper presents an experimental investigation of the effect of the damage degree and location on the static behavior and shear capacity of stud shear connectors. Numerical analysis was executed to simulate push-out tests and was validated with the test results. A parametric study was also performed to investigate the damage degree and location on the shear capacity of the studs based on the proposed numerical model. Finally, a theoretical formula supplemented with a reduction factor K was proposed to consider the reduction of the shear capacity due to the initial damage and was verified using experimental results.

2. Experimental program

2.1 Test specimens

Six push-out test specimens, as shown in Fig. 1 and as described Table 1, were designed to investigate the effect of the damage degree and location on the static behavior and load-slip characteristic at the interface of the shear connector between steel and concrete. Specimen TJ1 served as a standard specimen without damage. Specimens TJ2, TJ3 and TJ4 were fabricated with damage at the same location, where the distance from the stud root to the

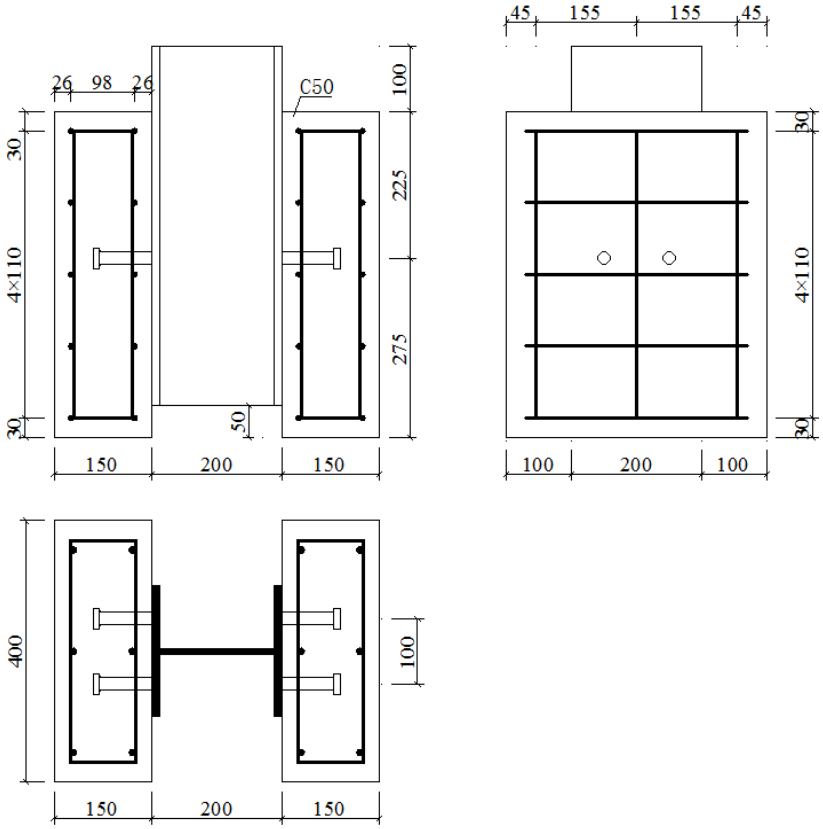

Fig. 1 Details of specimens

Table 1 Stud properties and test variables

Specimen	Specification (mm×mm)	Distance from stud root to damage section (mm)	Degree of damage	Test parameter
TJ1	19×80	/	/	Standard specimen
TJ2	19×80	9	A(12.8%)	Damage degree
TJ3	19×80	9	B(36.6%)	Damage degree
TJ4	19×80	9	C(62.9%)	Damage degree
TJ5	19×80	34	B(36.6%)	Damage location
TJ6	19×80	9 and 34	B(36.6%)	Multi damage

*Note: *A* = 3 mm damage depth; *B* = 7 mm damage depth; *C* = 11 mm damage depth

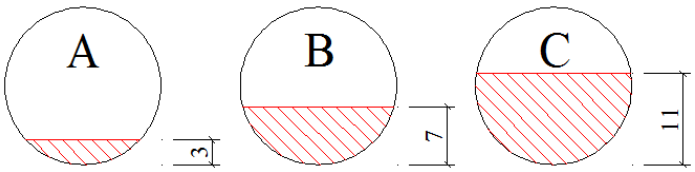

(a) Damage degree

(b) Manufacturing process

Fig. 2 Damaged studs

Table 2 Material properties of concrete

Series	Cylinder compression strength f_c' (MPa)	Young's modulus E_c (GPa)	Corresponding specimens
1	54.4	35.2	TJ1
2	56.4	35.5	TJ2, TJ3, TJ4
3	58.0	35.7	TJ5, TJ6

damage location was 9 mm, and various damage degrees on their shanks (i.e., damage depths of 3, 7 and 11 mm). Specimens TJ5 and TJ6 had damage in different locations.

All of the 6 push-out test specimens had the same dimensions: the thickness, width and height of concrete slab were 150 mm, 400 mm and 500 mm, respectively. Hot-rolled H steel was used as the steel beam based on Chinese code (GB/T11263-2010 2010). Hot-rolled plain bars that were 10 and 8 mm in diameter were embedded in the concrete slabs, resulting in a longitudinal reinforcement ratio of 0.785% and a lateral reinforcement ratio of 0.670%.

The layout of the damage locations was arranged on the tension side of shank, which was detrimental to the shear force resistance of the studs during the push-out testing procedure. Fig. 2(a) shows the damage degrees of the specimens. Three degrees of damage were designed: levels A, B and C, which corresponded to damage depths of 3, 7 and 11 mm, respectively. As shown in Fig. 2(b), the stud was initially fixed, and the damage location was determined. The cutting speed was reduced when the depth of the saw approached the damage depth, and the damage depth was measured to ensure that the error in the damage depth was within ±0.5 mm.

2.2 Material properties

Three series of concrete cylinder specimens that were used in the various tests of this study were prepared for compressive strength tests at the time that the push-out specimens were cast. Table 2 summarizes the material properties of the concrete used in this study. Longitudinal

Table 3 Material properties of reinforcement

Diameter d (mm)	Yield strength f_y (MPa)	Tensile strength f_u (MPa)	Young's modulus E_s (GPa)
8	312.5	471.8	195
10	390.2	458.5	195

Table 4 Material properties of headed studs

Stud dimension (mm×mm)	Yield strength f_y (MPa)	Tensile strength f_u (MPa)	Elongation rate (%)
19×80	400.6	494.6	26

reinforcement was provided by 10 mm-diameter mild steel bars with average yield strength of 390.2 MPa, while mild steel bars with a nominal diameter of 8 mm with an average yield strength of 312.5 MPa were used for transverse reinforcement (Table 3). The yield strength, tensile strength and elongation rate of the headed stud are shown in Table 4.

Fig. 3 View of the test setup

(a) TJ1

(b) TJ2

(c) TJ3

(d) TJ4

(e) TJ5

(f) TJ6

Fig. 4 Failure mode of specimens

2.3 Testing and loading instrumentation

As shown in Fig. 3, the push-out specimens were tested in a computer-controlled electro-hydraulic servo tension/ compression testing machine with a capacity of 5000 kN The jack load was imparted to the specimen through the reaction force of the rising steel bearing. To ensure a uniform load application, the web of the steel beam near the loading point was polished, and a steel plate was placed between the reaction frame and the top of the specimen. In

addition, a layer of fine sand was spread on the surface of the steel bearing to guarantee a uniform load transfer.

A preloading was first applied in increments up to 10% of the expected failure load to examine the proper functioning of the machine. The loading rate of the formal loading process was initially 1/30 of the expected failure load and was then transformed into a displacement load with a loading rate of 0.01 mm/s when the interlayer slip between the concrete and steel was 1 mm. The longitudinal slip was measured, and the propagation of the crack was recorded at each loading step.

3. Test results and discussion

3.1 Mode of failure and shear strength

As was demonstrated in many previous studies, three failure modes would typically occur in push-out test specimens, including concrete failure where no stud failure was observed, shank failure without concrete failure and combined failure of the stud and concrete slab (Xue *et al*. 2008, Lam and EI-Loboby 2005). In this experimental study, only shank failure was observed in all specimens with different cut off sections. Fig. 4 shows the failure mode of all six specimens for which the photograph of the steel surface and concrete surface at the ultimate state is shown. It is shown that the weakest section was the root of the shank in the normal specimens (e.g., TJ1 and TJ2) but was at the damage location in the damaged specimens (e.g., TJ3, TJ4, TJ5 and TJ6). Note that for specimen TJ2, of which the damage degree was not severe, the root of the shank instead of damage location was cut off, indicating a significant stress at the end of the stud when the damage degree was not severe.

Table 5 summarizes the ultimate shear capacity, characteristic slip and failure mode of the test specimens. S_u represents the slip when the applied load reached its peak value and S_{max} is defined as the ultimate slip. Based on the test results, the following findings can be derived:

- A reduction of up to 36.6% of the area of the shank did not significantly influence the shear strength of the test specimens, while a reduction of 62.9% of the area of the shank lead to a significant decrease in the shear strength of the studs.
- The damage location on the shank did not lead to a decline in the shear strength of the studs when the damage degree for the shank was less than 36.6%.

3.2 Load-slip curves and shear stiffness

Fig. 5 shows the dimensionless load-slip curves of the specimens. The shear load is shown as a proportion of the maximum applied load, while the interlayer slip is shown as a proportion of the shank diameter. The tested load-slip curves consist of three different stages: a linear elastic portion, a plastic portion and a descending portion. In the elastic portion, the shear connectors exhibit similar behaviors with linear relationships between the imposed load and the interlayer slip up to approximately 60% of the maximum load. In the plastic portion, the load-slip curves show a softened behavior with decreased shear stiffness. The slip increases significantly, while no increase in the applied load is observed; the shear stiffness also approaches zero when the load approaches the ultimate load. After the ultimate load is achieved, the specimens fail suddenly with a steep and short load-slip in the descending portion of the curve.

The ratios of the ultimate slip to the shank diameter for all of the specimens except specimen TJ4 were primarily located at approximately 0.35, which is similar to the test results of Oehlers and Xu (Oehlers and Coughlan 1986, Xu *et al*. 2012) with regard to the ratio of approximately 1/3. For specimen TJ4, this ratio was only 0.12, which was probably due to a premature failure of the shank.

Because small amounts of slip are typically difficult to detect, and any of these measurements typically have low precision, the stiffness of the stud connector is defined as

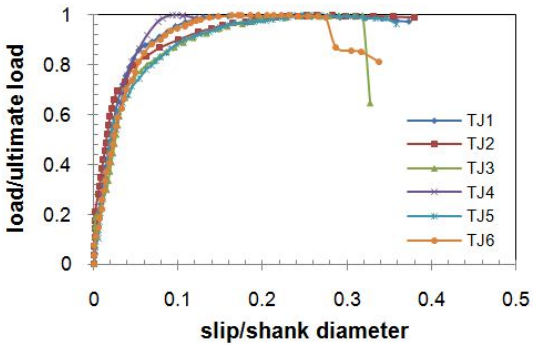

Fig. 5 Dimensionless load-slip curves

Table 5 Experimental result of test specimens

Specimen	Ultimate strength per stud P_u (kN)	Dropping rate† (%)	S_u (mm)	S_{max} (mm)	Failure mode
TJ1	145.4	0	6.03	7.08	Shank failure (root)
TJ2	143.7	-1.2	5.37	7.22	Shank failure (root)
TJ3	134.8	-7.9	4.33	6.21	Shank failure (root and damage location)
TJ4	92.5	-57.2	1.78	2.27	Shank failure (damage location)
TJ5	147.3	1.3	5.24	6.8	Shank failure (root and damage location)
TJ6	135.8	-7.1	3.89	6.41	Shank failure (root and damage location of 9 mm)

† Rate of decrease in the maximum shear strength to that of specimen TJ1

Table 6 Shear stiffness of test specimens

Specimen	k_1 (kN/mm)		k_2 (kN/mm)			
	Test	FEM	Test	Rate of decrease † (%)	FEM	Rate of decrease † (%)
TJ1	207.0	187.1	68.8	0	60.4	0
TJ2	289.9	202.3	68.3	0.7	60.1	0.5
TJ3	181.7	198.9	59.6	13.4	58.4	3.3
TJ4	146.4	181.1	46.1	33.0	53.9	10.8
TJ5	205.5	202.8	65.7	4.5	60.5	-0.2
TJ6	176.2	197.4	63.8	7.3	58.0	4.0

*Note: k_1 corresponds to the shear stiffness at a slip of 0.2 mm; k_2 corresponds to the shear stiffness at a slip of 2 mm; † rate of decrease of the shear stiffness to that of specimen TJ1

the load at a relative slip of 0.2 and 2 mm, as shown in Table 6. It is shown that no significant regularity is found in the shear stiffness at the 0.2 mm relative slip due to measurement errors. Conversely, typical regularity is obtained for the shear stiffness at the 2 mm relative slip:

- The shear stiffness decreased as the damage degree increased. Reductions of 0.7%, 13.4% and 33.0% in the shear stiffness were observed in the specimens with damage degrees of 12.8%, 36.6% and 62.9%, respectively.
- The damage location in the specimens with a damage degree of 36.6% had no significant influence on the shear stiffness.

4. Finite element analysis

4.1 General

Finite element analysis is an efficient tool to simulate the behavior of push-out tests that could remedy deficiencies in the quantity and quality of test specimens. Some pioneering researchers have made significant contributions to the field of numerical simulations relating to various finite element packages, including ABAQUS, DIANA, etc. (Lam and EI-Loboby 2005, Xu *et al*. 2012, Okada *et al*. 2006). In this study, ANSYS was selected to simulate the behavior of the test specimens of interest. Before FEM investigation, a verification study based on the test results was performed to ensure the reliability of the following parametric study.

Many factors tend to affect the accuracy of numerical simulations include the material constitution, element type, mesh technology, contact interaction, boundary condition, loading manner, etc. Consequently, these technological measurements should be carefully considered before a formal FEM study is performed.

4.2 Establishment of FEM model

Considering the symmetry of the dimensions, boundary conditions, loading mechanisms and computational efficiencies, half of each specimen was simulated. In the simulation model, three-dimensional eight-node nonlinear elements (Solid65) were used to simulate the concrete, and three-dimensional eight-node isoparametric elements (Solid45) were used to simulate the steel plate and studs, while three-dimensional spar elements (link8) were used to simulate the embedded reinforcements.

The simulation model was assembled using concrete, rebar, studs and steel plate and set based on mechanical

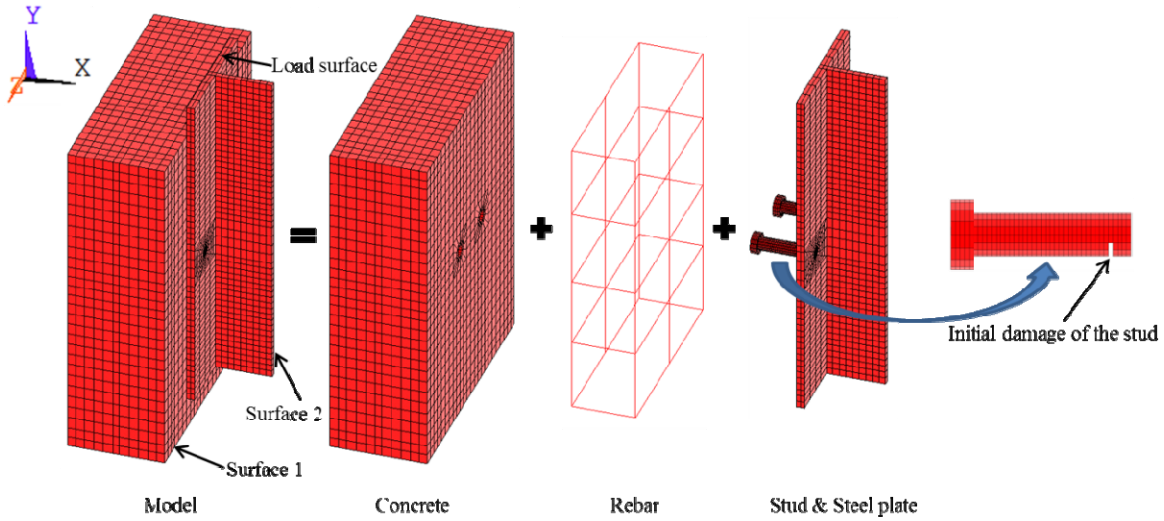

Fig. 6 FEM model

symmetrical regulation, as shown in Fig. 6. The bottom concrete surface, called surface 1, was restrained from moving in all three directions. The steel beam web surface, called surface 2, was considered to be symmetric across the X-axis, meaning that all nodes along this surface cannot move along the X axis.

The loading surface, which sustained a static concentrated load, is shown in Fig. 6. To obtain a stable and reliable solution, the load application rate should be carefully designated and sufficiently slow to prevent a dramatic increase in the kinematic energy. The optimum loading rate was set to be 0.02 mm/s by using the trial and error approach of different loading rates.

Sliding could be occurred at the contact surfaces between the concrete slabs and the steel flanges and between the stud shanks and surrounding concrete, which should be simulated by contact analyses. In the FEM model, the contact surfaces of the steel flanges and the stud shanks

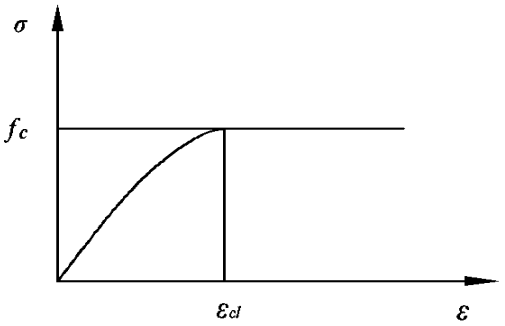

Fig. 7 Stress-strain curve of the concrete

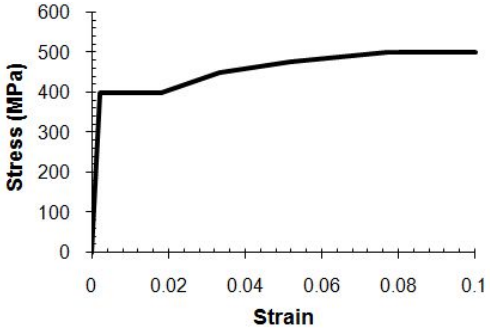

Fig. 8 Stress-strain curve of the stud

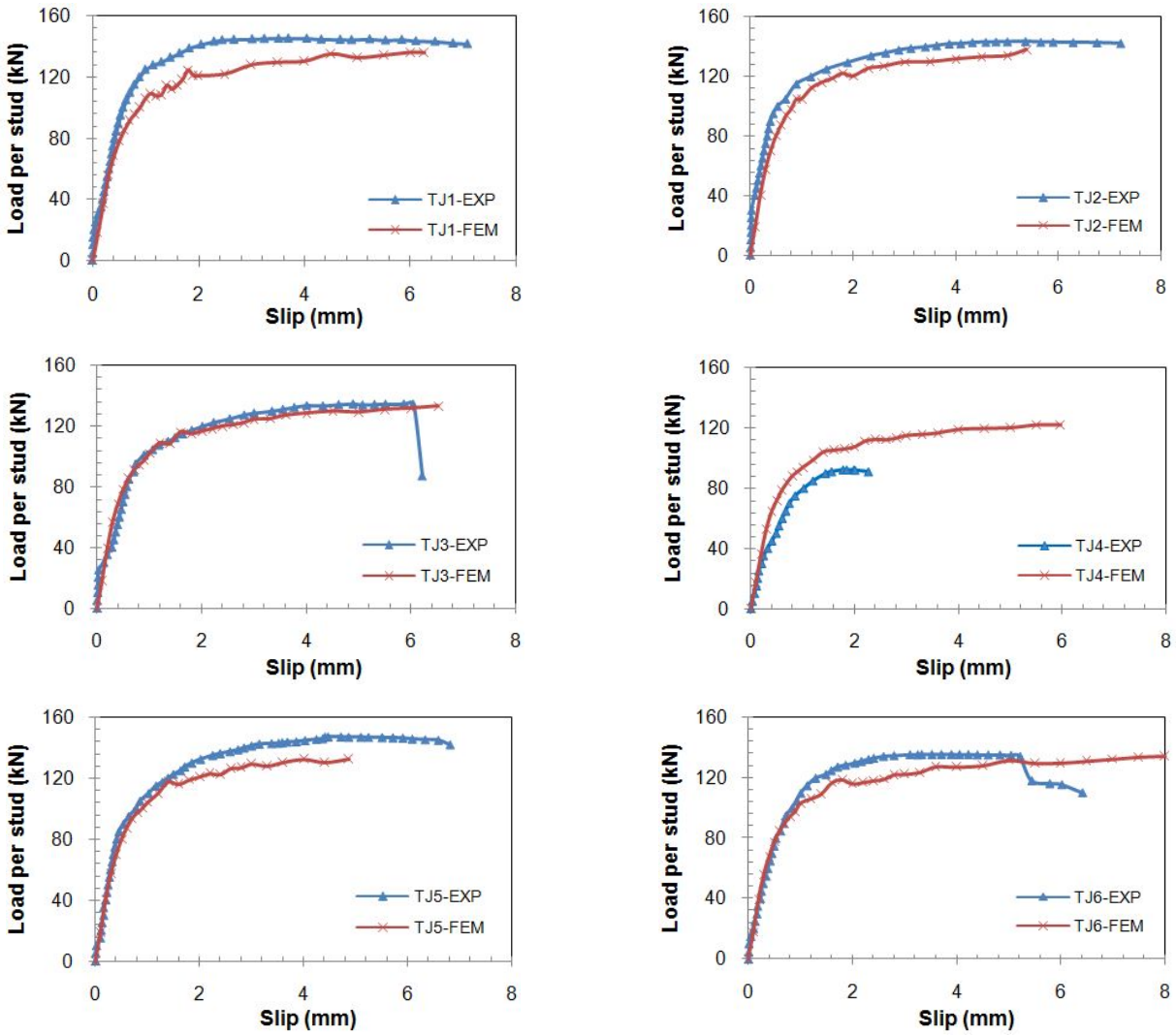

Fig. 9 Comparison of the load-slip curves from the test results and the FEM model results

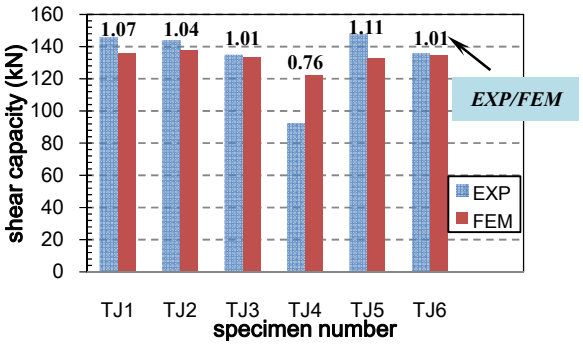

Fig. 10 Comparison of the shear capacities from the test results and the FEM model results

stud shanks were defined as contact elements that were simulated by conta174 elements, and the concrete contact surfaces were selected as target segment elements that were simulated by targe170 elements. The friction coefficient between the interlayer faces was assumed to be 0.3, which was equal to the value adopted by Xu *et al*. (2012). The initial damage of the stud was simulated by killing the element corresponding to the portion removed from the real stud.

As to material constitution, the concrete was treated as an elastic-plastic material and neglected the descending stages due to hardly handling on local crushing of concrete underneath stud shank for FEM analysis, as shown in Fig. 7. This stress-strain relationship was explicitly expressed by the following equation

$$\frac{\sigma_c}{f_c} = \frac{k\eta - \eta^2}{1 + (k-2)\eta} \tag{1}$$

where f_c is the concrete compressive strength; σ_c is the stress in the concrete; $\eta = \varepsilon_c/\varepsilon_{c1}$; ε_{c1} is the strain at maximum stress; and k can be referred to as EC2 and $k = 1.05E_c \times \varepsilon_{c1}/f_c$. Fig. 8 shows the stress-strain curve for the stud that was modeled using a multi-linear model based on experimental tensile tests.

4.3 FEM analysis and verification

Fig. 9 shows the comparison between the load-slip curves obtained experimentally and those produced by the numerical simulation for each specimen. The FEM verification results achieved good correlation with the test results except for specimen TJ4, which was probably due to rapid experimental load rate or a weld defect, which resulted in delayed load transfer from the stud to the concrete and thus the damage section on the shank. Consequently, it is believed that the proposed FEM method has sufficient accuracy to simulate the push-out tests and to execute the following parametric study.

The shear capacities of the test specimens predicted by the FEM model and the test results are compared in Fig. 10. The FEM prediction shows good agreement with the experimental results; however, the shear capacities predicted by the FEM analysis was smaller than those found experimentally. As shown in Table 6, the shear stiffness at a slip of 0.2 mm was inordinate, while typical regularity was obtained at the 2 mm relative slip in the FEM analysis results. An increased damage degree was found to lead to a reduction in the shear stiffness; however, the damage location showed no significant influence on the shear stiffness.

Fig. 11 shows the Von Mises stresses of all test specimens at ultimate load. The stress mainly concentrated in the minimum section when the damage section located near the stud root. The shear capacity and shear stiffness are determined by the area of the minimum section. However, significant influence was not found when the damage section located far away from the stud root which was in accordance with the test results.

The results of the comparison indicated that the FEM model was reliable for the subsequent parametric study of the mechanical behavior of damaged studs.

5. Parametrical study

To accurately evaluate the influence of the initial

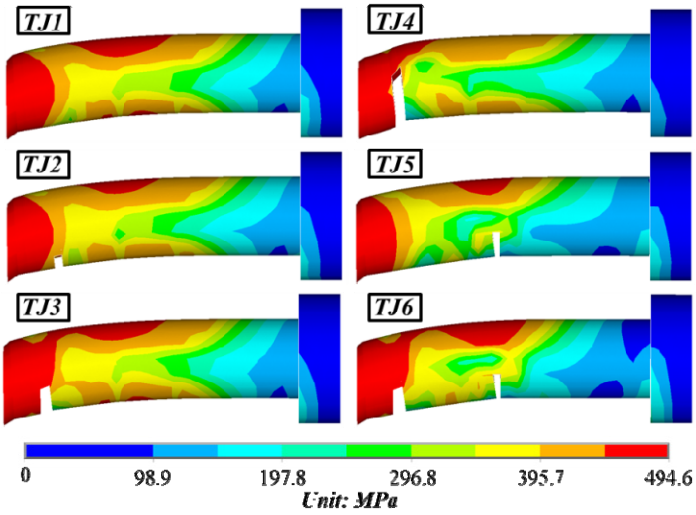

Fig. 11 Von Mises stresses of studs at ultimate state

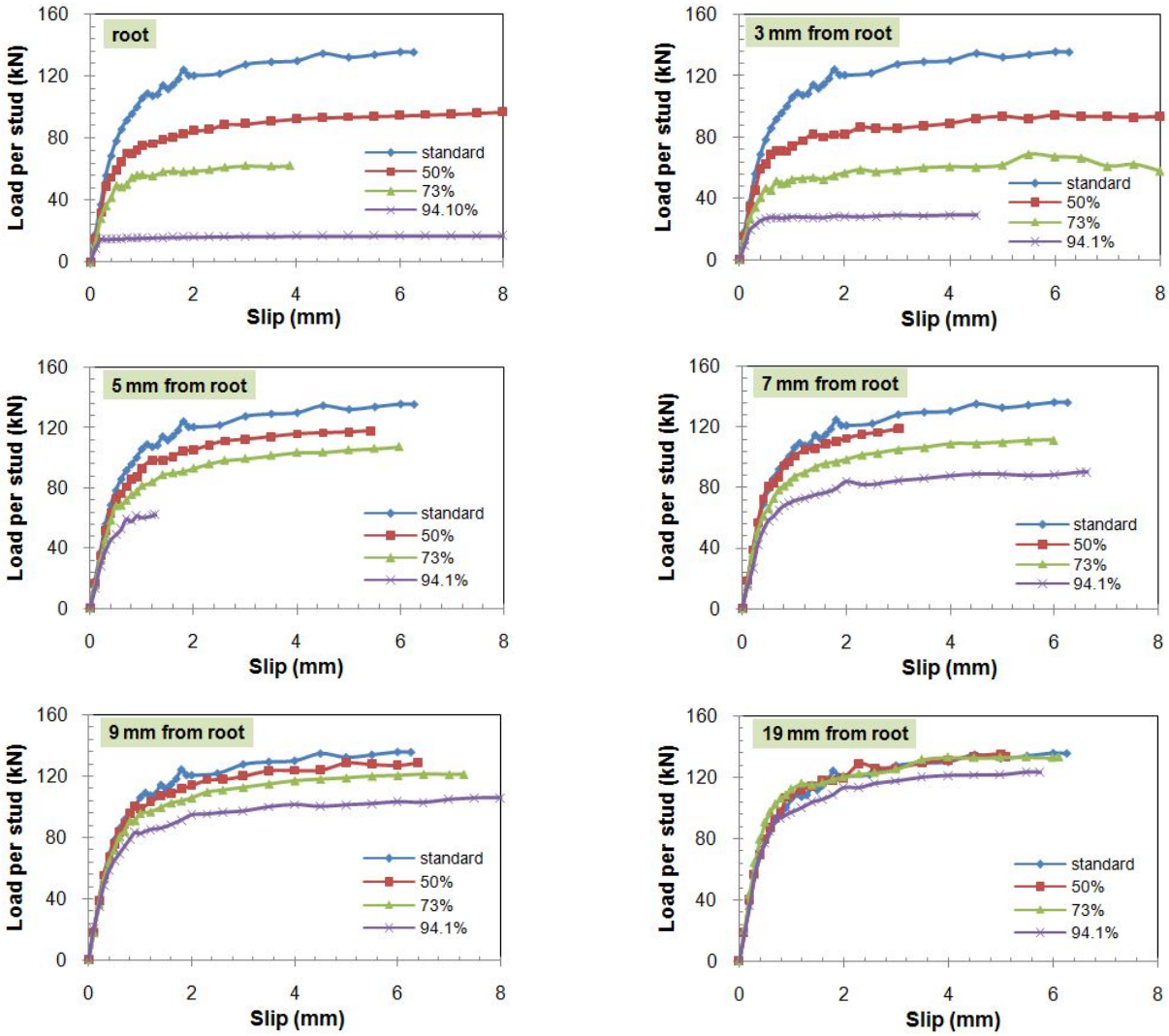

Fig. 12 Load-slip curves for studs with various damage degrees and different damage locations

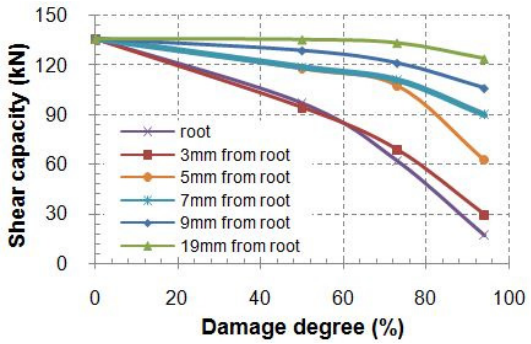

Fig. 13 Parametric analysis of the stud shear capacity with different damage degrees

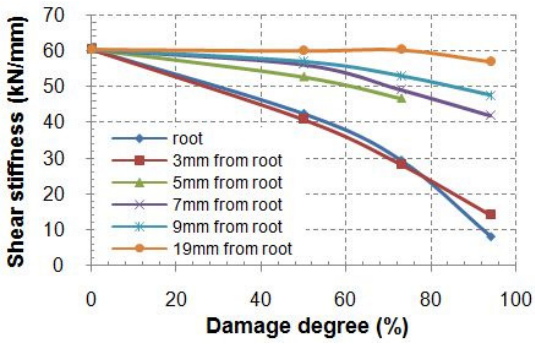

Fig. 14 Parametric analysis of the stud shear stiffness with different damage degrees (2 mm slip)

damage on the stud shank's ultimate capacity, a parametric study based on the standard specimen TJ1 was conducted using the proposed FEM model with two parameters: the damage degree and the damage location. The damage degree is defined as the reduction in the stud shank area, and the damage location is the distance from the damage section to the root of the shank. Four damage degrees, which were 0% (i.e., the standard specimen), 50%, 73% and 94.1%, were selected in this parametric study because a slight damage degree (i.e., less than 50%) had no significant influence on the stud shear capacity when the damage location was far from the root according to FEM analysis results. Damage locations of 0, 3, 5, 7, 9 and 19 mm (i.e., from the root to the location of the damage) were

investigated simultaneously because a real damage location usually occurred near the root in engineering practice.

Figs. 12 and 13 respectively show the load-slip curves for the various damage degrees with different damage locations and the parametric analysis of the stud shear capacity with different damage degrees. It can be concluded from these figures that as the damage degree increases, the shear capacity decreases; this influence also becomes more significant for specimens with shorter damage locations. It is interesting to note that shear capacity is also shown to be insensitive to the damage degree when the damage location is 0.5d, where d is the shank diameter, from the stud root even if the stud has experienced a significant reduction in area. That is to say damage to the stud could be neglected when the distance from the damage location to root is larger than 0.5d.

Fig. 14 shows parametric analysis of the stud shear stiffness with different damage degrees at the 2 mm relative slip. The shear stiffness is shown to decrease as the damage degree increases, particularly for specimens with damage locations nearer to the root.

6. Shear capacity of studs with initial damage

Many unpredictable types of damage could appear on shear connectors, including shank corrosion, fatigue, mechanical defects, weld defects, etc. Engineering practice teaches us that most damage occurs at the region near the stud roots. Fig. 15 shows the effect of the damage location on the shear capacity in the FEM results. Although the ultimate capacity increases as the damage location (i.e., the distance from the root to the location of the damage) increases, it is believed that using the shear strength calculated with root damage as the ultimate capacity is reasonable because this value is a conservative and safe estimation for different damage locations under a given damage degree.

As the previous parametric study showed, the initial damage of a stud would result in a reduction in its shear capacity and tend to be more observable in specimens with larger damage degree. However, the influence of the initial damage on the stud shank's ultimate capacity is not considered in the existing theoretical calculation methods and the current specifications, which include Eurocode 4 (EC4 1994 1994), AASHTO LRFD (2014) and GB50017-2003. Therefore, a reasonable calculation method that can consider the reduction in capacity of shear connectors should be established to evaluate the shear capacity of studs.

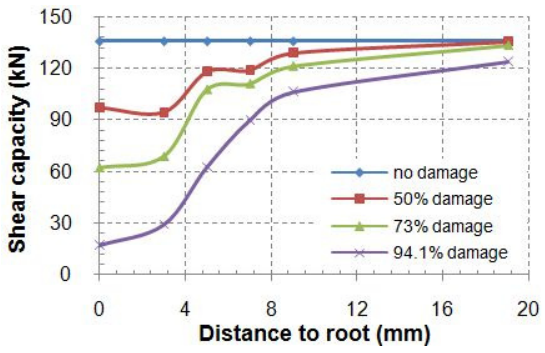

Fig. 15 Shear capacity versus damage location

In this study, a two-level concept for stud shear capacity in which the initial damage of a stud is considered is proposed. In this concept, a reduction factor K is introduced into the proposed method to consider the effect of the damage degree on the shear capacity of the stud; thus, the design shear capacity of stud can be expressed as follows

$$P_{Rd} = K \min(P_{stud}, P_{concrete}) \tag{2}$$

where P_{stud} and $P_{concrete}$ are the shear capacity dominated by "stud failure" and that dominated by "concrete failure", respectively, which could be calculated using the expression of an undamaged stud. The remaining issue is to determine the formula for the reduction factor K.

Based on intuition, a linear relationship is likely between the shear capacity reduction factor and the damage degree; this can be specified as one principle of judgment on the effect of the initial damage on the shear capacity. However, the stress state of a damaged stud differs from that of an integrated stud, which probably results in a diverse relationship between the shear capacity reduction factor and the damage degree. Consequently, a nonlinear squared relationship that corresponds to the diameter of the stud, which is set as another principle of judgment on the effect of initial damage on shear capacity, is assumed. Thus, the reduction factor satisfies a linear relationship with a nominal diameter of the remaining stud area after transferring it to an intact circle.

6.1 Reduction factor K—Level 1

In the Level 1, a linear relationship for K and η is used based on the intuition that the shear bearing capacity is proportional to the stud area. The failure mode estimation is based on Eurocode 4 (EC4 1994 1994). For stud failure, K is determined by the following equation:

$$K = 1 - \eta \qquad f_{ck} \geq 4.69 f_u^2 / \alpha^2 E_{cm} \tag{3a}$$

For concrete failure, K is expressed as follows:

$$K = \begin{cases} 1 & \eta < K_c \\ 1 - \dfrac{\eta - K_c}{1 - K_c} & \eta \geq K_c \end{cases} \qquad f_{ck} < 4.69 f_u^2 / \alpha^2 E_{cm} \tag{3b}$$

where η is the damage degree and is specified by the ratio of the removed area to total area of a stud; f_{ck} is the compressive strength of the concrete cylinders; f_u is the ultimate tensile strength of the stud; E_{cm} is the Young's modulus of the concrete; $\alpha = 0.2(h_{sc} / d + 1) \leq 1$, where h_{sc} is the overall height of stud; d is the shank diameter of the stud; and K_c is the critical damage degree, which is calculated as follows

$$K_c = 1 - 0.46\alpha \sqrt{f_{ck} E_{cm}} / f_u \tag{4}$$

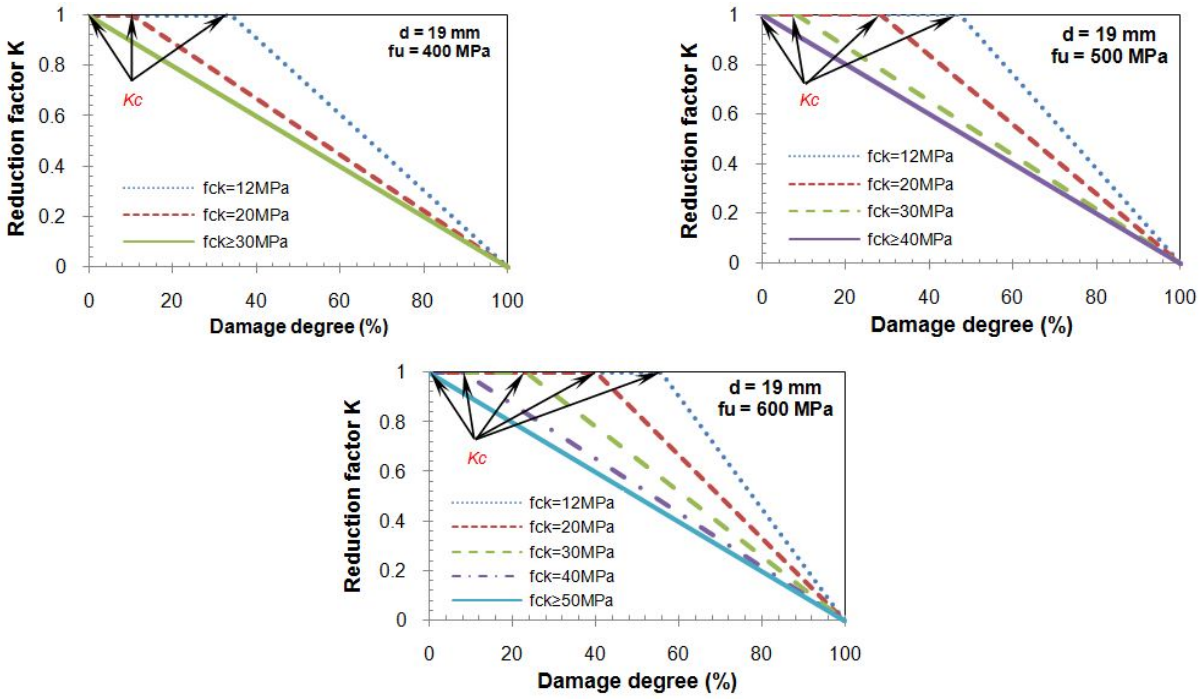

Fig. 16 Reduction factor K (Level 1)

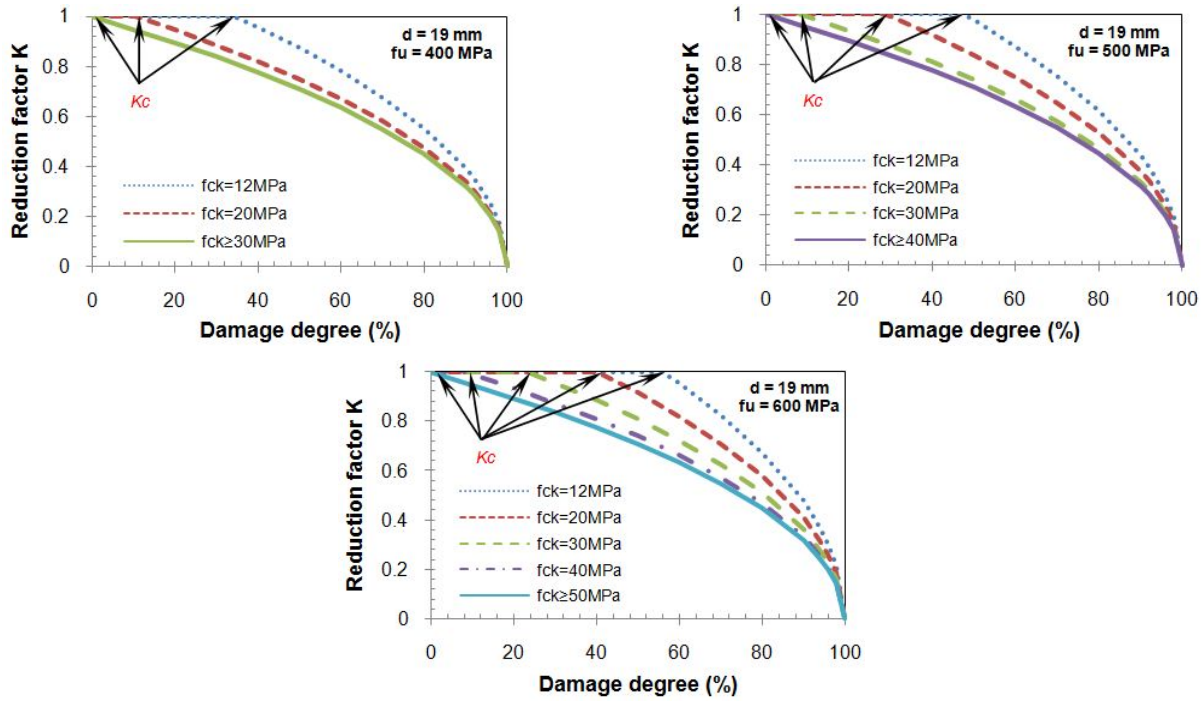

Fig. 17 Reduction factor K (Level 2)

As shown in Fig. 16, the reduction factor decreases as soon as the damage degree begins to increase during "stud failure", while the reduction factor maintains a value of 1 and decreases as the damage degree increases beyond the critical damage degree for those cases of "concrete failure".

6.2 Reduction factor K—Level 2

In Level 2, a nonlinear squared relationship is assumed between the shear bearing capacity and the stud area. This relationship changes to become linear between the reduction factor and the nominal diameter of stud. Therefore, for stud failure, K is calculated as follows

$$K = \sqrt{1-\eta} \qquad f_{ck} \geq 4.69 f_u^2 / \alpha^2 E_{cm} \tag{5a}$$

For concrete failure, K is determined by the following equation

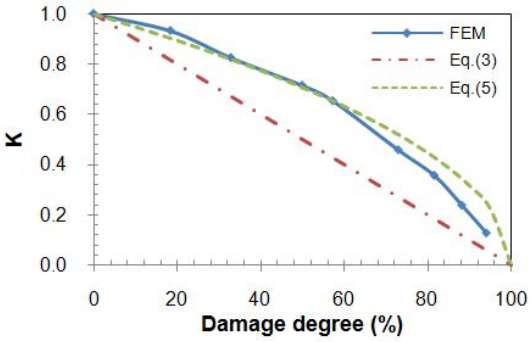

Fig. 18 Comparison of the proposed reduction factor K and the FEM results

$$K=\begin{cases}1 & \eta < K_c \\ 1-\sqrt{\dfrac{\eta-K_c}{1-K_c}} & \eta \geq K_c \end{cases} \quad f_{ck} < 4.69 f_u^2/\alpha^2 E_{cm} \qquad (5b)$$

Fig. 17 shows that K decreases slowly at lower damage degrees, while a significant decrease is observed at higher damage degrees. To demonstrate the reliability of Eqs. (3) and (5), a comparison between the proposed reduction factor and the FEM results based on the previous parametric study is performed, as shown in Fig. 18. It is shown that Eq. (5) correlates well with the FEM results, confirming the validity of the assumption of a linear relationship between the reduction factor and the nominal diameter of the damaged stud.

6.3 Verification

Table 7 lists the observed stud shear capacities of the experimental results in the references and of the related design values of the proposed method based on several design specifications. Table 8 shows the comparisons of the ratios of the calculated values to the measured values.

As shown in Tables 7 and 8, the shear capacity predictions of Level 1 were more conservative than those calculated in Level 2, indicating that Level 2 was more accurate in evaluating the ultimate capacity of stud shear connectors. With different specifications, the calculated results based on AASTHO and GB50017-2003 showed better agreement with the experimental results, corresponding to the mean value of the ratio of the calculated values to the measured values; these ratios were equal to 0.868 and 0.870 for Level 1 and 0.937 and 0.934 for Level 2 with standard deviations of 0.141, 0.198, 0.072 and 0.143, respectively, while Eurocode 4 (EC4 1994 1994) provided an over-conservative prediction for the test specimens. Thus, the proposed method of Level 1 could be applied to design purpose which could provide a more safety result while Level 2 is recommended for the purpose of precise prediction of shear capacity.

It can be concluded that if the exact damage degree of the shear stud connector no matter due to corrosion, fatigue or weld defect can be detected by nondestructive inspection method, for example ultrasonic wave method, the ultimate capacity can be predicted and the safety of the real bridge can be evaluated by the proposed approach. In another perspective, the shear capacity of an integrated stud, locates in the position that is more likely to be damaged, can be

Table 7 Calculated results

References	Specimen	Measured value	Eurocode 4				AASHTO				GB50017-2003			
			P_{stud}	$P_{concrete}$	Level 1	Level 2	P_{stud}	$P_{concrete}$	Level 1	Level 2	P_{stud}	$P_{concrete}$	Level 1	Level 2
This study	TJ1	145.4	112.2	150.7	112.2	112.2	140.2	204.1	140.2	140.2	121.2	171.1	121.2	121.2
	TJ2	143.7	112.2	154.2	97.8	104.8	140.2	208.8	122.3	131.0	121.2	175.0	105.7	113.2
	TJ3	134.8	112.2	154.2	71.1	89.3	140.2	208.8	88.9	111.7	121.2	175.0	76.9	96.5
	TJ4	92.5	112.2	154.2	41.6	68.3	140.2	208.8	52.0	85.4	121.2	175.0	45.0	73.8
	TJ5	147.3	112.2	157.0	71.1	89.3	140.2	212.5	88.9	111.7	121.2	178.1	76.9	96.5
	TJ6	135.8	112.2	157.0	71.1	89.3	140.2	212.5	88.9	111.7	121.2	178.1	76.9	96.5
Rong *et al.* (2013)	S1-1	115.3	84.9	98.0	84.9	84.9	106.2	132.7	106.2	106.2	124.1	111.2	111.2	111.2
	S1-2	112.5	84.9	98.0	84.9	84.9	106.2	132.7	106.2	106.2	124.1	111.2	111.2	111.2
	S1-3	112.3	84.9	98.0	84.9	84.9	106.2	132.7	106.2	106.2	124.1	111.2	111.2	111.2
	S2-1	110	84.9	99.6	79.7	82.3	106.2	134.9	99.7	102.9	124.1	113.0	106.1	109.5
	S2-2	99.8	84.9	99.6	79.2	82.0	106.2	134.9	99.0	102.5	124.1	113.0	105.4	109.1
	S2-3	108.9	84.9	99.6	83.5	84.2	106.2	134.9	104.3	105.2	124.1	113.0	111.1	112.1
	S3-1	93	84.9	99.6	69.6	76.9	106.2	134.9	87.0	96.1	124.1	113.0	92.7	102.4
	S3-2	97	84.9	99.6	70.4	77.3	106.2	134.9	88.0	96.7	124.1	113.0	93.7	102.9
	S3-3	98	84.9	99.6	71.9	78.1	106.2	134.9	89.9	97.7	124.1	113.0	95.7	104.0
	S4-1	110	84.9	97.4	84.9	84.9	106.2	131.9	106.2	106.2	124.1	110.5	110.5	110.5
	S4-2	108.5	84.9	97.4	84.9	84.9	106.2	131.9	106.2	106.2	124.1	110.5	110.5	110.5
	S4-3	111.3	84.9	97.4	84.9	84.9	106.2	131.9	106.2	106.2	124.1	110.5	110.5	110.5

Table 8 Comparisons of calculated and measured values

References	Specimen	Eurocode 4		AASHTO		GB50017-2003	
		Level 1	Level 2	Level 1	Level 2	Level 1	Level 2
This study	TJ1	0.772	0.772	0.964	0.964	0.834	0.834
	TJ2	0.681	0.729	0.851	0.911	0.736	0.788
	TJ3	0.528	0.663	0.660	0.828	0.570	0.716
	TJ4	0.450	0.739	0.562	0.923	0.486	0.798
	TJ5	0.483	0.606	0.604	0.758	0.522	0.655
	TJ6	0.524	0.658	0.655	0.822	0.566	0.711
Rong *et al*. (2013)	S1-1	0.737	0.737	0.921	0.921	0.965	0.965
	S1-2	0.755	0.755	0.944	0.944	0.989	0.989
	S1-3	0.756	0.756	0.945	0.945	0.990	0.990
	S2-1	0.725	0.748	0.906	0.935	0.965	0.996
	S2-2	0.793	0.822	0.992	1.027	1.056	1.094
	S2-3	0.766	0.773	0.958	0.966	1.020	1.029
	S3-1	0.749	0.827	0.936	1.034	0.997	1.101
	S3-2	0.726	0.797	0.907	0.996	0.966	1.061
	S3-3	0.734	0.797	0.917	0.997	0.977	1.061
	S4-1	0.772	0.772	0.965	0.965	1.005	1.005
	S4-2	0.783	0.783	0.978	0.978	1.019	1.019
	S4-3	0.763	0.763	0.954	0.954	0.993	0.993
Mean		0.694	0.750	0.868	0.937	0.870	0.934
SD		0.113	0.057	0.141	0.072	0.198	0.143

*Note: Mean = mean value; SD = standard deviation

reduced to a considerable level by estimating the damage degree according to engineering experience in the design process.

7. Conclusions

- Based on the test results in this study, under the condition of static load, a reduction of up to 36.6% in the area of the shank produced no significant effect on the shear capacity of the studs, while a reduction of 62.9% in the area of the shank lead to a significant decrease in the shear capacity of the studs. These results corresponded to a decrease in the maximum shear strength of 7.9% and 57.2% compared to the standard specimen. The damage location on the shank did not produce a decrease in the shear strength of the studs when the damage degree of the shank was less than 36.6%.
- The test results indicated that the shear stiffness at a 2 mm relative slip decreased as the damage degree increased. Reductions of 0.7%, 13.4% and 33.0% in the shear stiffness were observed in the specimens with damage degrees of 12.8%, 36.6% and 62.9%, respectively. The damage location in specimens with a damage degree of 36.6% had no significant influence on the shear stiffness of the studs.
- Based on the FEM analysis results, the shear capacity is shown to be insensitive when the damage section is 0.5*d*, where d is the shank diameter, from the stud root even if the stud has experienced a significant reduction in area.
- A theoretical formulation with a reduction factor *K* is proposed to consider the reduction in the shear capacity of the stud due to its initial damage. Two different principles of determining the expression of *K* are recommended. *K* is assumed to satisfy a linear relationship with the damage degree, while a nonlinear squared relationship is assumed between the shear bearing capacity and the stud area, indicating that *K* has a linear relationship with the nominal diameter of the stud. The proposed method showed good agreement with the experimental results and was convenient, relatively fast and thus relevant for use in engineering design.

Acknowledgments

This study was supported by the National Key R&D Plan (2017YFC07034). The financial support of this Program is significantly appreciated.

References

AASHTO (2014), Bridge Design Specifications; American Association of State Highway and Transportation Officials, Washington, DC, USA.

EC4 1994 (1994), Design of composite steel and concrete structures.

GB/T11263-2010 (2010), Hot rolled H and cut T section steel; Beijing, China.

GB50017-2003 (2003), Code for design of steel structures; Beijing, China.

Goble, G.G. (1968), "Shear strength of thin flange composite specimens", *Eng. J.*, **5**(2), 62-65.

Han, Q., Wang, Y., Xu, J., Xing, Y. and Yang, G. (2017), "Numerical analysis on shear stud in push-out test with crumb rubber concrete", *J. Constr. Steel Res.*, **130**, 148-158.

Hiragi, H., Matsui, S. and Fukumoto, Y. (1989), "Derivation strength equations of headed stud shear connectors-static strengths", *Struct. Eng.*, **35**(3), 1221-1232.

Lam, D. and EI-Loboby, E. (2005), "Behavior of Headed Stud Shear Connectors in Composite Beam", *J. Struct. Eng.*, **131**(1), 96-107.

Liu, Y. and Alkhatib, A. (2013), "Experimental study of static behaviour of stud shear connectors", *Can. J. Civil Eng.*, **40**(9), 909-916.

Ju, X. and Zeng, Z. (2015), "Study on uplift performance of stud connector in steel-concrete composite structures", *Steel Compos. Struct., Int. J.*, **18**(5), 1279-1290.

Nie, J.G. and Cai, C.S. (2003), "Steel–Concrete Composite Beams Considering Shear Slip Effects", *J. Struct. Eng.*, **129**(4), 495-506.

Oehlers. D.J. (1989), "Splitting induced by shear connectors in composite beams", *J. Struct. Eng.*, **115**(2), 341-362.

Oehlers. D.J. and Coughlan, C.G. (1986), "The shear stiffness of stud shear connections in composite beams", *J. Constr. Steel Res.*, **6**(4), 273-284.

Oehlers D.J. and Park, S.M. (1992), "Shear connectors in composite beams with longitudinally cracked slabs", *J. Struct. Eng.*, **118**(8), 2004-2022.

Okada, J., Yoda, T. and Lebet, J.P. (2006), "A study of the grouped arrangements of stud connectors on shear strength behavior", *Struct. Eng./Earthq. Eng.*, **23**(1), 75s-89s.

Ollgaard, J., Slutter, R.G. and Fisher, J.W. (1971), "The strength of stud shear connection in lightweight and normal-weight concrete", *Eng. J.*, **8**(2), 55-64.

Pallarés, L. and Hajjar, J.F. (2010), "Headed steel stud anchors in composite structures, Part I: Shear", *J. Constr. Steel Res.*, **66**(2), 198-212.

Pathirana, S.W., Uy, B., Mirza, O., Mirza, O. and Zhu, X.Q. (2015), "Strengthening of existing composite steel-concrete beams utilising bolted shear connectors and welded studs", *J. Constr. Steel Res.*, **114**, 417-430.

Rong, X.L., Huang, Q. and Ren, Y. (2013), "Experimental study on static and fatigue behaviors of stud connectors for composite beams after corrosion", *China Civil Eng. J.*, **46**(2), 10-18. [In Chinese]

Salari, M.R., Shing, P.B. and Frangopol, D.M. (1998), "Nonlinear analysis of composite beams with deformable shear connectors", *J. Struct. Eng.*, **124**(10), 1148-1158.

Slutter, R.G. and Driscoll, G.C. (1965), "Flexural strength of steel concrete composite beams", *J. Struct. Div.*, **91**(2), 71-99.

Su, Q., Yang, G. and Bradford, M.A. (2014), "Static behaviour of multi-row stud shear connectors in high-strength concrete", *Steel Compos. Struct., Int. J.*, **17**(6), 967-980.

Viest, I.M. (1956), "Investigation of stud shear connectors for composite concrete and steel T-beams", *ACI J.*, **27**(8), 875-981.

Xing, Y., Han, Q., Xu, J., Guo, Q. and Wang, Y. (2016), "Experimental and numerical study on static behavior of elastic concrete-steel composite beams", *J. Constr. Steel Res.*, **123**, 79-92.

Xu, C. and Sugiura, K. (2013), "Parametric push-out analysis on group studs shear connector under effect of bending-induced concrete cracks", *J. Constr. Steel Res.*, **89**, 86-97.

Xu, C., Sugiura, K., Wu, C. and Su, Q.T. (2012), "Parametrical static analysis on group studs with typical push-out tests", *J. Constr. Steel Res.*, **72**, 84-96.

Xu, C., Sugiura, K., Masuya, H., Hashimoto, K. and Fukada, S. (2014), "Experimental study on the biaxial loading effect on group stud shear connectors of steel-concrete composite bridges", *J. Bridge. Eng.*, **20**(10), 04014110. DOI: 10.1061/(ASCE)BE.1943-5592.0000718

Xue, W.C., Ding, M., Wang, H. and Luo, Z.W. (2008), "Static behavior and theoretical model of stud shear connectors", *J. Bridge Eng.*, **13**(6), 623-634.

Xue, D., Liu, Y., and Yu, Z. and He, J. (2012), "Static behavior of multi-stud shear connectors for steel-concrete composite bridge", *J. Constr. Steel Res.*, **74**, 1-7.

CC